# Quaternary Raised Coral-Reef Terraces on Sumba Island, Indonesia

P. A. Pirazzoli, U. Radtke, W. S. Hantoro, C. Jouannic, C. T. Hoang, C. Causse, M. Borel Best

**A spectacular sequence of coral-reef terraces (six steps broader than 500 meters and many minor substeps) is developed near Cape Laundi, Sumba Island, between an ancient patch reef 475 meters high and sea level. Several raised reefs have been dated with the electron spin resonance and the uranium-series dating methods. The uplift trend deduced from these reefs is 0.5 millimeter per year; most terraces, although polycyclic in origin, appear to correspond to specific interglacial stages, with the oldest terrace formed 1 million years ago. This puts them among the longest and most complete mid-Quaternary terrace sequences.**

Sequences of raised marine terraces have been reported from many coastal areas worldwide. The best examples are found in the Huon Peninsula (Papua New Guinea) and Barbados (West Indies) and are used as Quaternary reference data to trace past sea-level changes and interglacial periods. In the Huon Peninsula, geological observations and Th-U dating (*1*) allowed an assessment of eustatic fluctuations until 150 ka (*2*) and, by correlation with O isotope records, this range was extended to 250 ka (*3*). In Barbados, marine chronology was clarified after U-series dating of corals until isotope stage 5e (*4*), then extended to stage 15 by correlation with O isotope chronology and a combination of $^{230}Th$-$^{234}U$ and He-U dating (*5*), and application of the electron spin resonance (ESR) method (*6, 7*). Recently, the precision of age estimates up to 130 ka was significantly improved with the mass spectrometric Th-U method (*8*). In the Indonesian region, coral-reef terraces on Atauro Island, north of Timor, were dated with the Th-U method (*9*); fossil corals of the last interglacial period were used, and the dates were extended by correlation until 700 ka.

P. A. Pirazzoli, Laboratoire de Géographie Physique, Centre National de la Recherche Scientifique, 1 Place A. Briand, 92190 Meudon-Bellevue, France.
U. Radtke, Geographisches Institut, Heinrich-Heine Universität, 4000 Düsseldorf, Germany.
W. S. Hantoro, Laboratoire de Géologie du Quaternaire, Centre National de la Recherche Scientifique, Luminy, Case 907, 13288 Marseille Cedex 9, France, and Research and Development Centre for Geotechnology, Indonesian Institute of Sciences, Jalan Cisitu 21/154D, Bandung 40135, Indonesia.
C. Jouannic, Institut Français de Recherche Scientifique pour le Développement en Coopération (ORSTOM), Département TOA, 213 rue La Fayette, 75480 Paris Cedex 10, France, and Marine Geological Institute, Jl. Dr. Junsunan 236, Post Office Box 215, Bandung 40174, Indonesia.
C. T. Hoang, Centre des Faibles Radioactivités, Centre National de la Recherche Scientifique, et Commissariat à l'Energie Atomique, 91198 Gif-sur-Yvette Cedex, France.
C. Causse, Laboratoire d'Hydrologie et de Géochimie Isotopique, Université de Paris-Sud, Bâtiment 504, 91405 Orsay Cedex, France.
M. Borel Best, Nationaal Natuurhistorisch Museum, Post Office Box 9517, 2300 RA Leiden, Netherlands.

We describe in this paper a 1-million-year sequence of well-developed coral-reef terraces on Sumba Island, thus extending previously published records. The present set of two dozen $^{230}Th$ and ESR ages fulfills only in part the geochronological requirements. Although more analyses are needed, recent progress in refining the ESR dating technique on corals has allowed a reasonable age range for the terraces on Sumba Island to be estimated.

Raised terraces are geomorphologically well preserved near Cape Laundi (Fig. 1). Earlier work identified at least six major terraces, numbered I to VI (*10*). Most were subdivided into a number of substeps by scarps and alignments of reef ridges. It must have taken a long time for surfaces as wide as terraces III or II to form, as they are ten times as broad as the Holocene platform.

An α-counting U-series analysis, performed with the use of radiochemical procedures described in (*11*), indicated that U concentrations and $^{234}U/^{238}U$ activity ratios in the terraces were in the range of those generally observed in fossil corals. The $^{232}Th$ concentration is below or very close to the detection limit. The ESR method (*12*) has been applied to the same powder split of six samples ($I_2$LND.3, $I_2$MDL.4, $II_2$WTP.5, $II_2$MDL.10, $II_3$MDL.3, and $III_1$LND.3) used for U-series dating. The accumulated dose AD [unit: 1 gray (Gy)] was determined by the so-called "additive dose method" (*13*). Instrumental neutron activation analysis (INAA) and α-counting measurement of the U content in six samples show the same values for two samples and agreement within 2σ (95% confidence level) for the other cases (Table 1). A cosmic dose rate estimated at 150 μGy/year was added to the dose rate calculated from the U content.

For reef $IV_1$ (at +275 ± 10 m) (*14*) the ESR method gave two consistent results: 584 ± 88 and 603 ± 90 ka. Although 7 and 14% calcite were found in the samples, respectively, recrystallization seems to have only a limited effect on ESR results: samples with aragonite concentrations as low as 60% did not show a trend toward younger ages in Barbados, compared to samples with concentrations of 95 to 100% (*7*). Probably, therefore, terrace $IV_1$ was bioconstructed (at least partly) during isotopic stage 15, about 595 ± 22 ka (*15, 16*) (Fig. 2C). Three coral samples from reef $III_1$ (at +145 ± 10 m) were dated by ESR at 322 ± 48, 327 ± 49, and 397 ± 59 ka; the last age is supported by a date of >300 ka with the Th-U method. These data suggest that reef $III_1$ developed during isotopic stage 9 (about 330 ka). For the reef complexes of terrace II, the dates obtained are scattered over wide ranges: three dates between 228 ± 35 and 344 ± 52 ka for reef $II_3$ (at +62 ± 5 m) and six dates between 275 ± 41 and 117 ± 18 ka for reef $II_2$ (at +51 ± 6 m). The differences in age of about 100,000 years for shallow-water corals belonging to the same reefs with both the Th-U and ESR methods suggest that the terraces have a polycyclic origin. The sea returned at the same level several times. Because of the uplift trend, reef-crest corals in growth position on terrace surfaces were probably left by interglacial high sea levels

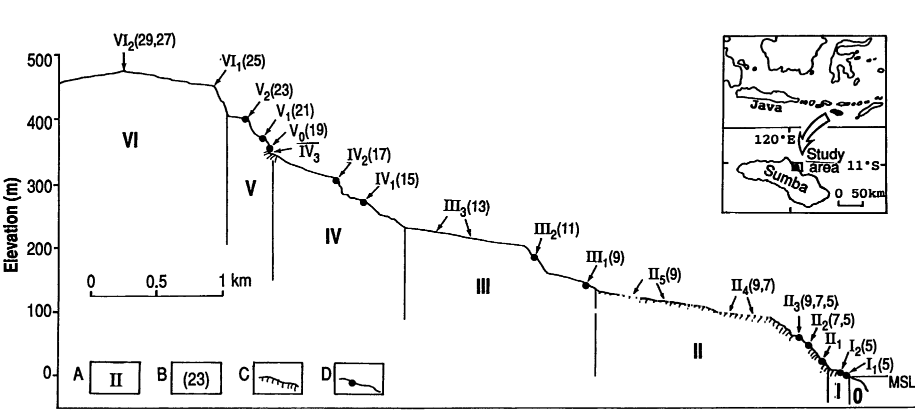


**Fig. 1.** Location map and simplified cross section along a reference transect, 5 km south of Cape Laundi: A, terrace identification; B, inferred O isotope stage; C, abraded surface; D, crest of raised reef.

not long before final emergence, whereas the age of underlying corals may represent other than interglacial times. Only scattered coral growth occurred during certain periods. For terraces $I_2$ (at +12 ± 7 m) and $I_1$ (at +5.0 ± 0.5 m), nine dates indicate that the coral reef developed during the last interglacial period. On the basis of comparisons between records deduced from 11 oceanic cores (*17*), it seems unlikely that sea level was higher than at present by more than a few meters during any interglacial of the past 2.5 million years.

A recently proposed time scale of O isotope records (*16*) was adopted for this comparison (Fig. 2, C and D). We assumed that during interglacial stages 5, 9, 11, and 25 the sea reached its present level (±5 m), whereas during stages 7, 13, 15, 19, and 21, when Holocene O isotope values were not attained, sea level may have been slightly lower (−12 ± 12 m) and during stages 17, 23, and 27 possibly even lower (−25 ± 25 m) (Fig. 2B).

The present-day elevation of reef $IV_1$ along the reference transect implies that the average uplift rate has been 0.48 ± 0.05 mm/year since 595 ± 20 ka; the elevation of reef-crest $III_1$ indicated that it has been uplifted at 0.44 ± 0.05 mm/year since 330 ka. We view these rates as rough estimates

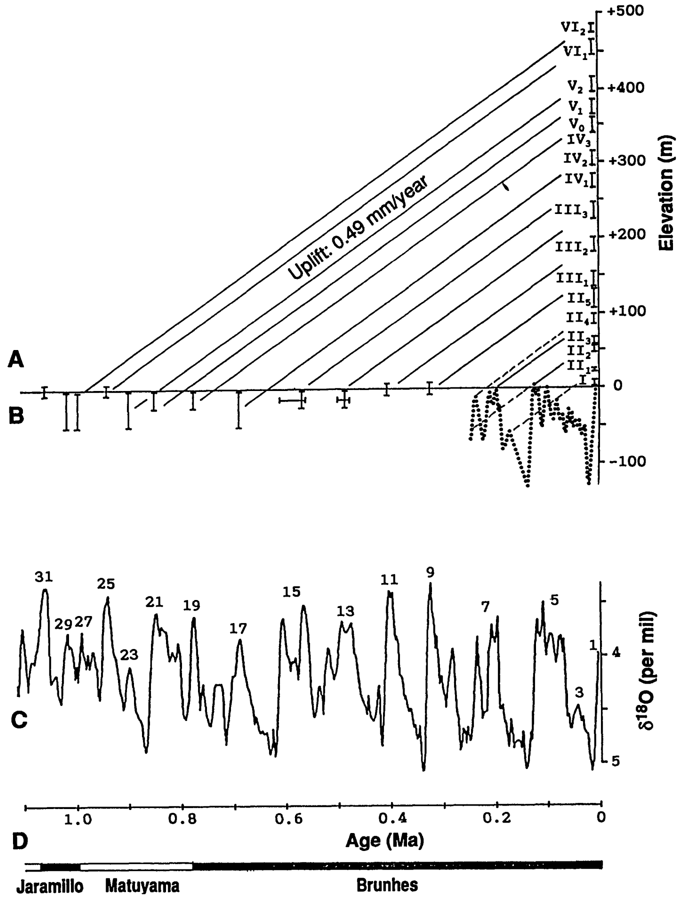


**Fig. 2.** Correlation between uplifted marine terraces, sea level, isotope stages, and paleomagnetism. (**A**) Model of uniform uplift rate. (**B**) Possible sea-level positions for the past 250 × $10^3$ years (*3*) and at previous interglacial peaks. (**C**) Astronomically calibrated benthonic isotope records from Ocean Drilling Program site 677 (*16*). (**D**) Revised paleomagnetic chronology (*16*).

**Table 1.** List of coral samples analyzed from the reef series of Cape Laundi, Sumba Island, Indonesia: sample codes, taxonomy, radiochemistry, and estimated ages. Uncertainty ranges correspond to 1σ. Coral species are as follows: *D h* = *Diploastrea heliopora* (Lamarck); *Fa p* = *Favia pallida* (Dana); *Fe* = *Favidae; Fs f* = *Favites flexuosa* (Dana); *G r* = *Goniastrea retiformis* (Lamarck); *O* = *Oulophylia; P* = *Porites* sp.; *Pl d* = *Platygyra daedaela* (Ellis and Solander); *Pl s* = *Platygyra sinensis* (Edwards and Haime); *Ps t* = *Pseudosiderastrea tayami* (Yabe and Sugiyama). We calculated the $^{230}Th$ ages using half-lives of $^{230}Th$ and $^{234}U$ of 75.2 × $10^3$ and 248 × $10^3$ years, respectively.

| Reef and sample | Coral species | Calcite (%) | U (ppm) | AD (Gy) | $^{234}U/^{238}U$ | $^{230}Th/^{234}U$ | $^{230}Th$ age (ka) | ESR age* (ka) |
|---|---|---|---|---|---|---|---|---|
| $O_1$ MDL.3 | *P* | 1 | 2.74 ± 0.07 | | 1.13 ± 0.02 | 0.056 ± 0.002 | 6.3 ± 0.2§ | |
| $I_1$ WTP.2 | *P* | <1 | 2.42 ± 0.07 | | 1.16 ± 0.04 | 0.537 ± 0.018 | 82 ± 4‡ | |
| $I_1$ MDL.1 | | <1 | 2.78 ± 0.06 | | 1.12 ± 0.03 | 0.732 ± 0.018 | 138 ± 9‡ | |
| $I_2$ LND.3 | *P* | 1 | 2.83 ± 0.07<br>2.45 ± 0.15† | <br>90.4 ± 4.0 | 1.12 ± 0.02 | 0.680 ± 0.020 | $120^{+8}_{-6}$§ | <br>119 ± 18 |
| $I_2$ MDL.8 | *Fs f* | 1 | 2.53 ± 0.15† | 117.3 ± 5.9 | | | | 142 ± 21 |
| $I_2$ MDL.11 | | <1 | 2.82 ± 0.07 | | 1.12 ± 0.01 | 0.728 ± 0.020 | $136^{+8}_{-7}$§ | |
| $I_2$ MDL.3 | *D h* | <1 | 2.55 ± 0.15† | 98.9 ± 4.4 | | | | 124 ± 19 |
| $I_2$ MDL.4 | *Ps t* | 1 | 3.52 ± 0.07<br>3.52 ± 0.21† | <br>88.7 ± 6.0 | 1.15 ± 0.02 | 0.666 ± 0.017 | 114 ± 7‡ | <br>93 ± 14 |
| $II_2$ WTP.5 | *Fa p* | <1 | 3.72 ± 0.10<br>3.52 ± 0.21† | <br>366.2 ± 32.4 | 1.10 ± 0.02 | 0.908 ± 0.027 | $237^{+31}_{-25}$§ | <br>275 ± 41 |
| $II_2$ MDL.10 | *P* | <1 | 3.00 ± 0.07<br>2.87 ± 0.17† | <br>100.9 ± 4.6 | 1.14 ± 0.01 | 0.720 ± 0.020 | 133 ± 7§ | <br>117 ± 18 |
| $II_2$ MDL.7 | | 1 | 3.59 ± 0.09 | | 1.06 ± 0.03 | 0.751 ± 0.023 | $148^{+14}_{-11}$‡ | |
| $II_2$ MDL.1 | *Fa (p?)* | 8 | 2.32 ± 0.14† | 206.3 ± 19.7 | | | | 232 ± 35 |
| $II_3$ MDL.1 | | 1 | 2.34 ± 0.07 | | 1.15 ± 0.04 | 0.908 ± 0.031 | $228^{+36}_{-26}$‡ | |
| $II_3$ MDL.3 | | 3 | 2.69 ± 0.07<br>2.50 ± 0.15† | <br>358.1 ± 18.5 | 1.11 ± 0.02 | 1.036 ± 0.032 | >300§ | <br>344 ± 52 |
| $III_1$ MDL.1 | *Pl s* | <1 | 2.61 ± 0.16† | 344.0 ± 14.3 | | | | 322 ± 48 |
| $III_1$ MDL.2 | *G r* | 6 | 1.53 ± 0.09† | 225.6 ± 12.6 | | | | 327 ± 49 |
| $III_1$ LND.3 | *Ps t* | 3 | 3.02 ± 0.08<br>3.02 ± 0.18† | <br>502.0 ± 51.0 | 1.07 ± 0.02 | 1.060 ± 0.030 | >300§ | <br>397 ± 59 |
| $IV_1$ LND.2 | *Fe? Pl? O?* | 7 | 2.21 ± 0.13† | 594.8 ± 44.2 | | | | 584 ± 88 |
| $IV_1$ LND.3 | *Pl d* | 14 | 2.83 ± 0.17† | 765.3 ± 69.1 | | | | 603 ± 90 |

*Uncertainty range estimated at ±15%. †Analyzed at INAA, Neutron test analysis, Hamilton, Ontario; uncertainty range estimated at 6%. ‡Analyzed by C.C. at the Laboratoire de Géologie du Quaternaire, Marseille. §Analyzed at Centre des Faibles Radioactivités, Gif-sur-Yvette.

only because some marine terraces are evidently capped by corals belonging to more than one interglacial stage and the precision of the ESR dates is estimated at ±15%. In addition, uplift rates may not have remained constant in time. Nevertheless, a check was made to discover whether a constant uplift rate could be found that would be consistent with most of the data available. Only unequivocal sea-level indicators, such as reef crests and notches, were used for correlation. Graphic attempts were made to find empirically whether a series of parallel uplift lines existed that would project past high sea levels, deduced from O isotope data and plotted with uncertainty ranges in Fig. 2A, into the vertical uncertainty ranges of sea-level indicators along the reference transect. The "best fitting" uplift rate is 0.49 ± 0.01 mm/year. At this rate, the elevation of the upper terrace ($VI_2$) corresponds to the superimposed effect of stages 27 and 29 and is therefore about 1 million years old. At the same uplift rate, most terrace elevations are consistent with certain interglacial stages ($VI_1$ with stage 25, $V_2$ with stage 23, $V_1$ with stage 21, $V_0$ and $IV_3$ with stage 19, $IV_2$ with stage 17; $IV_1$ is dated at stage 15; $III_3$ is consistent with stage 13, $III_2$ with stage 11; $III_1$ is dated at stage 9; the lower parts of $II_5$ and $II_4$ correspond to stage 7; $II_3$ was dated at stages 9 and 7 but was probably at sea level also during stage 5e; $II_2$ was dated at stages 7 and 5). Although the sea-level curve since 250 ka (Fig. 2B) may still be uncertain in some parts and slightly different from curves proposed by other investigators, it shows clearly that at an uplift rate of 0.5 mm/year superimposition of marine effects of different ages may occur at similar elevations.

In conclusion, Sumba Island terraces represent one of the longest series for mid-Pleistocene times. The close correlation between the raised marine sequence and the revised O isotope chronology (*16*) supports the reliability of this chronology for Quaternary studies. It also suggests that sea level was probably near to its present level at the maximum of stages 13 and 15 (O isotope values lower than the Holocene ones at these stages may be attributable to colder oceanic deep waters), possibly at −20 ± 10 m at stage 17, at −15 ± 10 m at stage 19, and between −25 and −40 m at stage 23.

ESR can be used to date older samples than α- or mass spectroscopy U-dating and is therefore the only tool that can be used today for a direct dating of mid- and early Pleistocene reef tracts. However, ESR is not precise enough to distinguish between interstadial substages. The spectacular sequence of marine terraces on Sumba Island make this an exceptionally favorable place to carry out new studies on the chemical, physical, isotopic, morphological, ecological, paleoclimatic, pedological, and diagenetic changes that have occurred during the past million years.


REFERENCES AND NOTES

1. J. Chappell, *Geol. Soc. Am. Bull.* **85**, 553 (1974); A. L. Bloom *et al. Quat. Res.* **4**, 185 (1974).
2. 1 ka = 1000 years ago.
3. J. Chappell and N. J. Shackleton, *Nature* **324**, 137 (1986).
4. K. J. Mesolella, R. K. Matthews, W. S. Broecker, D. L. Thurber, *J. Geol.* 77, 250 (1969).
5. M. L. Bender *et al.*, *Geol. Soc. Am. Bull.* **90**, 577 (1979).
6. M. Ikeya, *Nature* **255**, 48 (1975).
7. U. Radtke, R. Grün, P. Schwarcz, *Quat. Res. (N.Y.)* **29**, 197 (1988).
8. R. L. Edwards, J. H. Chen, T.-L. Ku, G. J. Wasserburg, *Science* **236**, 1547 (1987).
9. J. Chappell and H. H. Veeh, *Geol. Soc. Am. Bull.* **89**, 356 (1978).
10. C. Jouannic *et al.*, *Proc. 6th Int. Coral Reef Symp., Australia*, **3**, 441 (1988); W. S. Hantoro, C. Jouannic, P. A. Pirazzoli, *Photo Interprét.* **89** (no. 1), 17 (1989).
11. L. F. Montaggioni and C. T. Hoang, *Palaeogeogr. Palaeoclimatol. Palaeoecol.* **64**, 79 (1988); C. Causse and C. Hillaire-Marcel, in *Initial Reports, Ocean Drilling Program*, *B*, S. K. Stewart, Ed. (Government Printing Office, Washington, DC, 1989), pp. 551–560.
12. R. Grün, *Quat. Int.* **1**, 66 (1989).
13. ______ *et al.*, *Quat. Sci. Rev.*, in press.
14. Elevations, related to mean sea level, correspond to the upper surface of former reef crests along the reference transect.
15. J. Imbrie *et al.*, *North Atlantic Treaty Organization Adv. Study Inst. Ser. C* **126** (no. 1), 269 (1984).
16. N. J. Shackleton, A. Berger, W. R. Peltier, *Trans. R. Soc. Edinburgh Earth Sci.* **81**, 251 (1990).
17. N. J. Shackleton, *Quat. Sci. Rev.* **6**, 183 (1987).



20 December 1990; accepted 17 April 1991


# Development of Diapiric Structures in the Upper Mantle Due to Phase Transitions


M. Liu, D. A. Yuen, W. Zhao, S. Honda



**Solid-state phase transitions in time-dependent mantle convection can induce diapiric flows in the upper mantle. When a deep mantle plume rises toward phase boundaries in the upper mantle, the changes in the local thermal buoyancy, local heat capacity, and latent heat associated with the phase change at a depth of 670 kilometers tend to pinch off the plume head from the feeding stem and form a diapir. This mechanism may explain episodic hot spot volcanism. The nature of the multiple phase boundaries at the boundary between the upper and lower mantle may control the fate of deep mantle plumes, allowing hot plumes to go through and retarding the tepid ones.**


One of the striking features on the earth's surface is linear volcanic islands, such as the Hawaiian-Emperor chain in the Pacific. Morgan suggested (*1*) that these volcanic lineations were formed when plates move over relatively stationary hot regions, called hot spots, which are thought to result from deep mantle plumes.

An important feature of hot spot volcanism is the nature of the episodic eruptions and their role in the formation of discrete volcanoes along the chain. This manifestation suggests that mantle plumes are in the form of diapirs instead of continuous conduits. Such a notion is supported in part by surface wave studies from seismic tomography, which have found no continuous thermal anomalies at a depth of 300 km under the Hawaiian Islands (*2*).


M. Liu, Department of Geosciences, Pennsylvania State University, University Park, PA 16802.
D. A. Yuen and W. Zhao, Minnesota Supercomputer Institute and Department of Geology and Geophysics, University of Minnesota, Minneapolis, MN 55455.
S. Honda, Institute of Geology, Hiroshima University, 730 Hiroshima, Japan.


Some fluid dynamical mechanisms have been proposed to explain the generation of mantle diapirs. Deep mantle plumes may be sheared off by large-scale background circulation (*3*). Solitary wave disturbances (*4*) propagating within "mantle conduits" may also cause time-dependent plume behavior. In this report we describe mantle diapirs generated by the interaction between deep mantle plumes and polymorphic solid-state phase transitions in the upper mantle. Although temperature-dependent viscosity may be influential in mantle convection, other mechanisms, such as the effects of phase transitions on plumes, may also be important.

There are various mineral assemblages in the transition zone between depths of 350 and 700 km. Recent theoretical (*5*) and experimental (*6, 7*) work has established the major phase boundaries in the transition zone. Diapiric flows may be generated from the interaction of mantle flows with solid-solid phase transitions (*8*). These diapirs, which are isolated rising thermal anomalies, are generated from a rising plume as a result of changes in the local buoyancy, local heat